

Jana SMÉKALOVÁ*, Simona POSPÍŠILOVÁ**, Karel OBRTLÍK***,
Martin JULIS****, Tomáš PODRÁBSKÝ*****

FATIGUE CRACK INITIATION AND PROPAGATION IN COATED AND UNCOATED
INCONEL 713LC AT 800 °C

INICIACE A ŠÍŘENÍ ÚNAVOVÝCH TRHLIN V MATERIÁLU INCONEL 713LC BEZ VRSTVY
A S VRSTVOU PŘI TEPLITĚ 800 °C

Abstract

Fatigue crack initiation and propagation was studied in cast polycrystalline nickel base superalloy Inconel 713LC in as-received condition and with surface treatment by AlSi protective coating. Cylindrical specimens were cyclically strained under strain control with constant total strain amplitude at 800 °C. Fatigue fracture surface, specimen surface, and specimen sections were investigated using optical microscopy and scanning electron microscopy. Fatigue crack initiation sites and fatigue crack growth mechanisms were identified and crack propagation rates were obtained based on striation spacing in fracture surfaces. The crack initiation mechanism study revealed reasons for the fatigue life increase in the surface treated material.

Abstrakt

Tato práce je zaměřena na studium iniciace a šíření únavových trhlin u lité polykrystalické niklové superslitiny Inconel 713LC jak s ochrannou povrchovou vrstvou na bázi AlSi, tak bez vrstvy při teplotě 800 °C. Válcová zkušební tělesa byla cyklicky zatěžována za podmínek řízené deformace s konstantní amplitudou celkové deformace. Užitím optické a rastrovací elektronové mikroskopie byly analyzovány lomové plochy, povrch zatěžovaných vzorků a jejich osové řezy. Byla identifikována místa iniciace únavových trhlin a způsob jejich šíření a byla stanovena rychlost šíření na základě rozteče striací na lomových plochách. Studium mechanismu iniciace únavových trhlin odhalilo příčiny prodloužení únavové životnosti v materiálu s povrchovou úpravou.

1 INTRODUCTION

Nickel-based superalloys are used for high-temperature applications in power and aerospace industry. They are exposed to high temperatures fatigue and creep and their interactions, high-temperature oxidation and corrosion in aggressive environment, and erosion. The application of protective surface coatings (e.g. protective diffusion coatings) can result in the lifetime extension of strained parts and thus in increased performance of machines and structures. First of all the coatings provide the surface protection against the negative effect of environmental atmosphere.

Cast polycrystalline Ni-based superalloy IN713LC is used for gas turbine integral wheels and of auxiliary power units in aircraft industry. Its microstructure consists of γ matrix strengthened by ordered γ' phase. The precipitates $\text{Ni}_3(\text{Al,Ti})$ of the γ' phase are coherent to matrix (γ phase) with the

* Ing, Vysoké učení technické v Brně, Fakulta strojního inženýrství, Ústav materiálových věd a inženýrství, Technická 2896/2, Brno, e-mail janesmekalova@gmail.com

** Ing, Ph.D, Vysoké učení technické v Brně, Fakulta strojního inženýrství, Ústav materiálových věd a inženýrství Technická 2896/2, Brno, tel. (+420) 541 14 3148, e-mail pospisilova@fme.vutbr.cz

*** doc, RNDr, CSc, Akademie věd České republiky, v.v.i., Ústav fyziky materiál, Žižkova 22, Brno, tel. (+420) 532 290 341, e-mail obrtlik@ipm.cz

**** Ing, Ph.D, Vysoké učení technické v Brně, Fakulta strojního inženýrství, Ústav materiálových věd a inženýrství Technická 2896/2, Brno, tel. (+420) 541 14 3148, e-mail julis@fme.vutbr.cz

***** prof, Ing, CSc, Vysoké učení technické v Brně, Fakulta strojního inženýrství, Ústav materiálových věd a inženýrství, Technická 2896/2, Brno, tel. (+420) 541 14 3150, e-mail podrabsky@fme.vutbr.cz

face-centred cubic lattice. The precipitates having the $L1_2$ structure are stronger than the matrix at high temperatures. The morphology of the γ' precipitates in the alloy depends on the thermo-mechanical history [1]. Low cycle fatigue and high cycle fatigue of the material were studied rarely [2-6]. The diffusion coatings do not affect the creep life of Ni-based superalloys [7] but the effect on the fatigue life depends on number of factors [8,9]. Both the positive and detrimental effect of coatings was observed.

The aim of the present work is to study the fatigue crack initiation and propagation in superalloy IN713LC with AlSi protective coating and without coating at 800 °C. Fatigue crack propagation rates from striation spacing observed on fatigue fracture were correlated with the stress intensity factor. This work is a part of the complex research aimed at the influence of surface coatings on the fatigue behaviour of IN713LC [10].

2 EXPERIMENTAL DETAILS

The cast polycrystalline Ni-based superalloy IN713LC was provided by PBS, Velká Bíteš a.s. The chemical composition of the superalloy is the following: 0.05 hm% C; 12.08 hm% Cr; 0.75 hm% Ti; 5.91 hm% Al; 2.02 hm% Nb; 4.58 hm% Mo; < 0.05 hm% Mn, Co, Ta; rest Ni.

Low cycle fatigue tests were performed on button-end specimens having gauge length and diameter of 15 and 6 mm, respectively. The surface of the gauge length was prepared by polishing. The AlSi diffusion coating was applied to one series of specimens. The suspension of Al and Si was deposited on the gauge length using air pump spraying. Then, the specimens were annealed in protective argon atmosphere at 1000 °C for 3 hours, followed by slow cooling. The average total thickness of the coating varied from 40 to 55 μm . The other samples were used without the protected coating.

Specimens were fatigued in a computer controlled electro-hydraulic testing system at total strain rate of 0.002 s^{-1} with fully reversed total strain cycle ($R_\epsilon = -1$) at 800 °C in air. Selected parameters of low cycle fatigue tests of studied samples are shown in Tab. 1.

Tab. 1 Parameters of low cycle fatigue of studied samples

Sample	Total strain amplitude ϵ_a [%]	Number of cycles to fracture N_f	Stress amplitude σ_a [MPa]
3 coated	0.19	74 442	323.6
11 coated	0.24	9 178	407.3
4 coated	0.39	404	663.5
7 coated	0.52	244	725.7
A4 uncoated	0.18	35 001	310. 8
A2 uncoated	0.2	8 737	314. 7
A1 uncoated	0.26	8 660	389. 5
A8 uncoated	0.46	172	765.9

Based on previous research [9] it was found that the application of the AlSi protected coating has a positive effect on the lifetime of alloy Inconel 713LC. Fatigue crack initiation and propagation sites were studied by observing the fracture areas and surface cracks of coated and uncoated samples using light (LM) and scanning electron microscopy (SEM). The fatigue crack propagation rate was determined from the striation spacing in fracture surfaces.

3 EXPERIMENTAL RESULTS AND DISCUSSION

3.1 Fracture surface observation

The fracture surface of all studied samples is relatively rugged and not much corroded. The fatigue fracture and the final fracture could be easily distinguished - see Fig. 1 and 2. The casting defects, most often shrinkage pores (up to 0.9 mm in diameter) occurred in fracture surfaces. The oval-shaped area called fish eye (Fig. 1) was observed on fracture surfaces around some of the defects. It witnesses fatigue crack initiation and subsequent propagation in the area of these defects.

In all cases, the fatigue crack initiation was observed at the surface both of coated and uncoated samples (Fig. 1-3). In addition, fatigue cracks initiate and propagate from shrinkage pores inside the material.

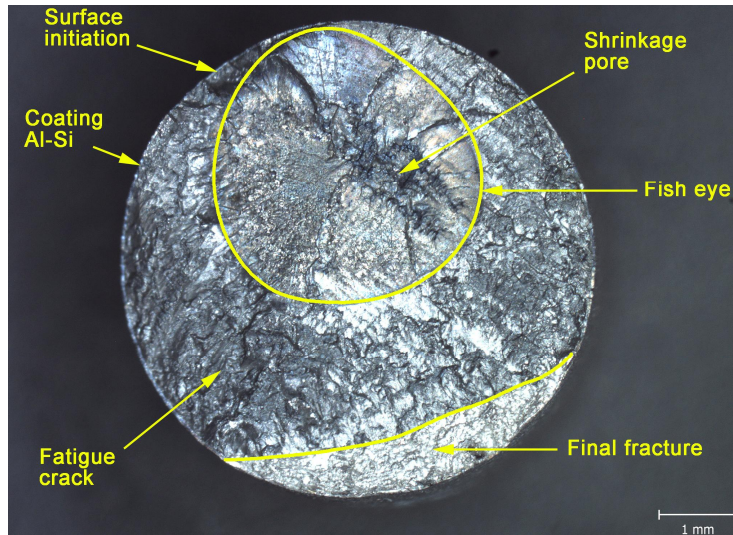


Fig. 1 The fracture surface of sample 3 with AlSi coating, $e_a = 0,19 \%$, LM

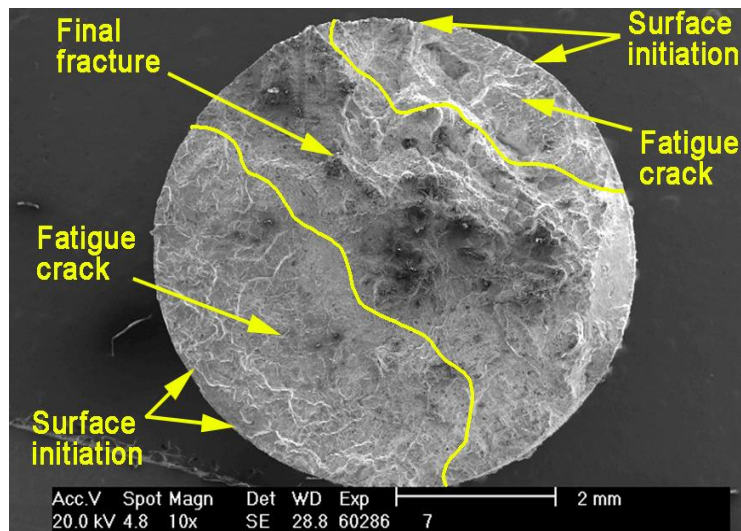


Fig. 2 The fracture area of sample 7 with AlSi coating, $e_a = 0,52 \%$, SEM

Striations were observed in fatigue fractures in all samples (Fig. 3b). They are typical for fatigue damage in the stage II of crack propagation. They were rarely observed also in fish eye areas. Comparatively high incidence of carbides (type MC) was observed both in the fatigue fracture and final fracture.

The number of initiated cracks increases with growing plastic strain amplitude (see Fig. 1 and Fig. 2).

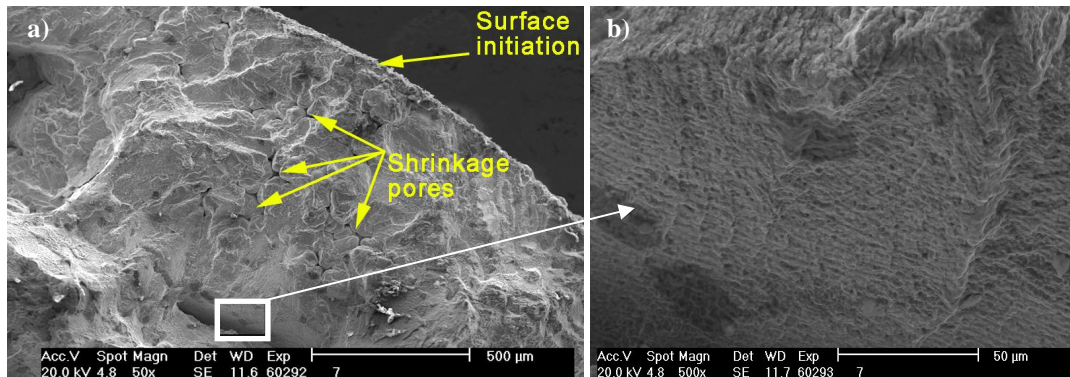


Fig. 3 a) Surface initiation near shrinkage pores, b) striations in fatigue fracture, sample 7 with AlSi coating, $e_a = 0,52\%$, SEM

3.2 Specimen surface and specimen section observation

Fig. 4 shows fatigue cracks on the sections parallel to the specimen axis at the end of the fatigue lifetime. Fig. 4a shows fatigue cracks that initiated at the sample surface, propagated through the protective coating AlSi and their propagation stopped in the substrate. Fatigue cracks initiated near the surface defects in the sample without protective coating are shown in Fig. 4b. After the domain of initial growth, the cracks propagate roughly perpendicularly to the specimen axis.

The concentration of fatigue cracks, initiated on the specimen surface, was higher in the coated material in all cases. In uncoated samples the surface cracks were observed only sporadically. Thus, the protected coating results in more homogeneous fatigue crack initiation. By contrast, high strain localization near the surface defects give rise to the low density of fatigue cracks in the uncoated material.

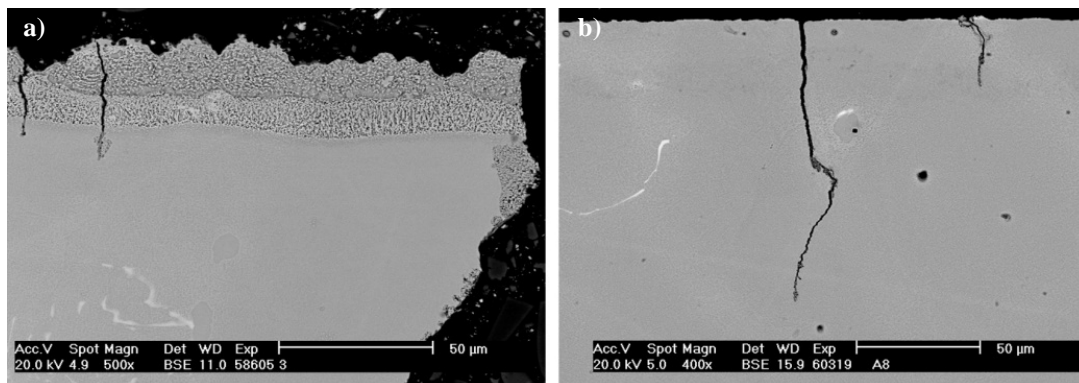


Fig. 4 a) Fatigue cracks on the section of sample 3 with coating AlSi, $e_a = 0,19\%$, SEM, b) fatigue cracks on the section of sample A8 without coating, $e_a = 0,46\%$, SEM

3.3 Evaluation of fatigue crack propagation rate

The fatigue crack propagation rate was obtained in the fish eye areas, from the outer edge of a defect to the border of the corresponding fish eye. In this area the crack shape was very well approximated by an ellipse. Fatigue crack propagation rate da/dN was determined by assuming that each striation corresponds to a load cycle. Then, the distance between neighbouring striations s is equal to da/dN . The crack length a is defined as the distance between the centre of the defect and the centre of a striation. N is the number of elapsed cycles.

Fatigue crack propagation rate was correlated with stress intensity factor range ΔK_I . To evaluate the stress intensity factor the linear elastic fracture mechanics was applied. First, it was verified that the stress intensity factor concept appropriately describes the stress state in the fish eye area. Recent results show that the value of plastic part of J-integral is negligible in material with similar mechanical properties using the total strain amplitude $\varepsilon_a = 0.20\%$, and therefore, it is possible to use linear elastic fracture mechanics [11]. Accordingly, specimens with the lowest total strain amplitudes were chosen to obtain the fatigue crack propagation rate; namely sample 11 with coating AlSi and sample A1 without coating. Further, the K-concept application was verified using relations (1) and (2) for the plastic zone size r_y , where S is the yield strength $R_{p0.2}$ of the alloy Inconel 713LC at 800 °C, K_{al} is the stress intensity factor amplitude and $S = pcb$ is the defect area approximated by an ellipse, where c and b are the major and minor ellipse axis, respectively. S_a is the remote stress amplitude.

$$r_y = \frac{1}{6p} \left(\frac{K_{al}}{S} \right)^2 \quad (1)$$

$$K_{al} = 0.5S_a \sqrt{p\sqrt{S}} \quad (2)$$

The plastic zone size is significantly smaller than the crack length or the ligament size in all cases. Therefore, the small scale yielding conditions are satisfied and the linear elastic fracture mechanics can be applied.

Fatigue crack propagation rate da/dN , estimated from striation spacing, versus the crack length a is shown in Fig. 5. The fatigue crack propagation rate da/dN is plotted vs. the stress intensity factor range ΔK in Fig. 6. The crack propagation data determined from striation spacing measurements of the present work (open symbols) were approximated using the Paris-Erdogan law,

$$\frac{da}{dN} = AK_{al}^m, \quad (3)$$

where material parameters $A = 8.9 \cdot 10^{-11} \text{ m cyclus}^{-1} (\text{MPa m}^{1/2})^{-m}$ and $m = 3.3$ were evaluated with regression analysis. K_{al} is the stress intensity factor amplitude for an elliptical crack in an infinite body. It was calculated using the following equations [12]

$$K_{al} = \frac{S_a \sqrt{p}}{E(k)} \cdot \sqrt{\frac{b}{c}} \cdot \sqrt[4]{(c^2 \sin^2(f) + b^2 \cos^2(f))} \quad (4)$$

$$E(k) = \frac{p}{2} \left[1 - \left(\frac{1}{2} \right)^2 k^2 - \left(\frac{3}{8} \right)^2 \frac{k^4}{3} - \left(\frac{15}{48} \right)^2 \frac{k^6}{5} \right], \quad k^2 = 1 - \left(\frac{b}{c} \right)^2. \quad (5)$$

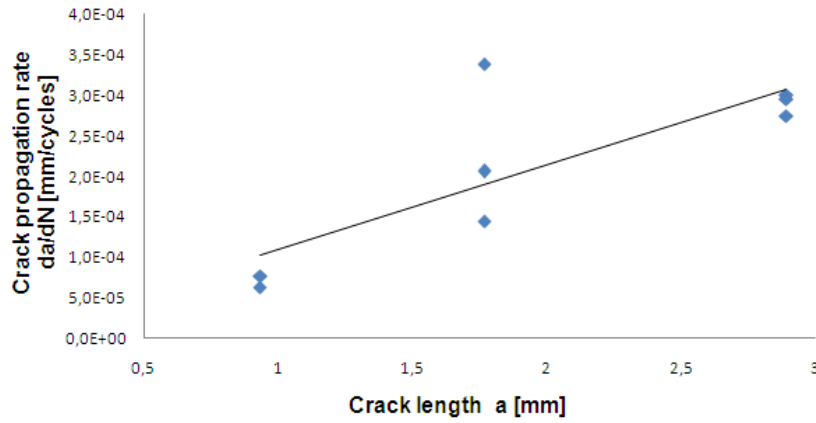


Fig. 5 Fatigue crack propagation rate vs. crack length, sample 3 with coating AISi, $e_a = 0,19\%$, SEM

It is noted that crack growth data found from striation spacing correspond well with literature data obtained in CT specimens of superalloy IN 713C at 600 °C at R=0 [13] (dashed line in Fig. 6). The crack propagation data of the present work are also in a good agreement to fatigue crack propagation rates of surface cracks acquired from cylindrical specimens at 600 °C [13].

Number of cycles necessary to elliptical crack extension from the initial size c_i (outer elliptic perimeter of a defect) to the final fish eye edge observed (size c_f) was estimated (equation (6)) based on the integration of the relation (3) using the material parameters found out in this work. Parameter $p = b/c$ in equation (6) is the ratio of the minor and major ellipse axis. The calculation shows that 916 cycles (10 % of fatigue life) are needed for crack propagation from the initial defect size to the fish eye border in specimen 11. Similarly, fatigue crack propagates 935 cycles (10.8 % of fatigue life) in specimen A1.

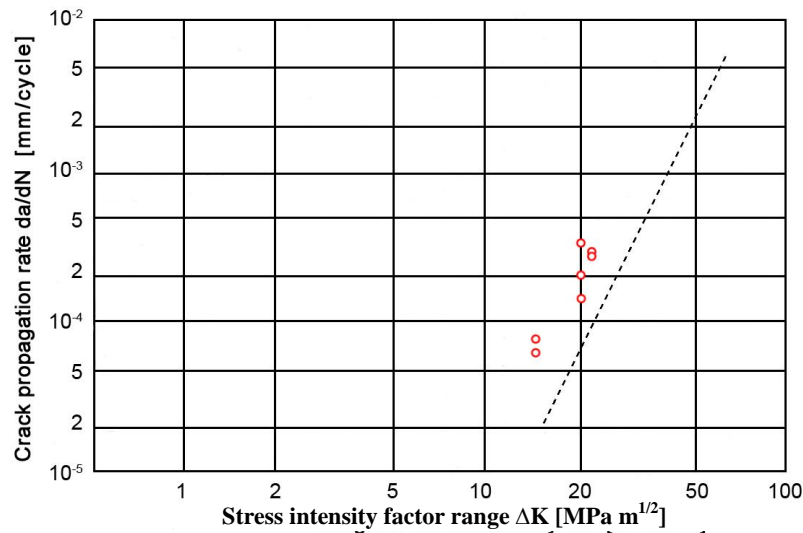


Fig. 6 Crack propagation rate vs. stress intensity factor range for material IN 713LC at 800 °C (open symbols, present work) and for material IN 713C at 600 °C (dash line, [12])

$$N = \frac{1}{A \cdot \left(s_a 0,5 \cdot \sqrt{p} \sqrt{p \cdot p} \right)^m} \left(\frac{c_f^{\frac{1-m}{2}} - c_1^{\frac{1-m}{2}}}{1 - \frac{m}{2}} \right) \quad (6)$$

Fig. 1 shows that defects present in IN 713LC are very rugged. The above calculation (equation (6)) shows that only small part of the fatigue life of specimens is spent in fatigue crack propagation from the crack corresponding to the elliptical circumference of a defect to its fish eye border. This finding suggests that the majority of fatigue life is occupied by crack initiation and early crack growth to the circumferential elliptic crack of the defect. On the other hand, previous literary data show that the crack growth rate obtained from striation spacing is several times higher than that from surface observation [14,15]. This information together with the fact that in the present study striations occupy only small portion of the fatigue fracture suggest that the number of cycles to crack propagation and to crack initiation and early growth to the elliptical circumference of a defect are more balanced.

4 SUMMARY AND CONCLUSION

- ❑ The fatigue crack initiation was observed on the free surface and also from inner defects (shrinkage pores) in both, coated and uncoated specimens. The crack propagation mechanism was transcrystalline.
- ❑ Low density of surface cracks in uncoated material is indicative of high strain localization near defects.
- ❑ Homogenous crack initiation corresponding to higher crack density leads to the fatigue life increase in the coated material.
- ❑ The fatigue crack propagation rates determined from striation spacing can be approximated by the Paris-Erdogan law.

REFERENCES

- [1] RATEL, N. & BASTIE, B.P. & MORI, T. *Acta Materialia*. 2006, Vol. 54, pp. 5087-5093.
- [2] OBRTLÍK, K. & MAN, J. & POLÁK, J. Room and high temperature low cycle fatigue of Inconel 713LC. In *EUROMAT 2001*. Rimini: Associazione Italiana di Metallurgia, 2001.
- [3] OBRTLÍK, K. et al. Cyclic strain localization in Inconel 713LC at room and high temperature. In *Fatigue 2002*. West Midlands: EMAS (A. F. Blom, Ed), 2002, pp. 963.
- [4] PETRENEC, M. & OBRTLÍK, K. & POLÁK, J. Inhomogeneous dislocation structure in fatigued Inconel 713LC superalloy at room and elevated temperatures. *Mater. Sci. Eng., A* 400-401 (2005) 485.
- [5] KUNZ, L. et al. Effect of mean stress on high-cycle fatigue strength of IN 713LC superalloy. *Metallic Mater.*, 44 (2006) 275.
- [6] RUSZ, S., ČÍŽEK, L., DOBRZAŇSKI, L.A., KEDROŇ, J. AND TYLŠAR, S. ECAP methods application on selected non-ferrous metals and alloys, *Archives of Materials Science and Engineering*, Vol. 43, June 2010, p. 69-76, ISSN 1897-2764
- [7] JULIŠ, M. & POSPÍŠILOVÁ, S. & PODRÁBSKÝ, T. An Application of Al-Si Layer on Nickel-based Superalloys and their Analysis. *Chemické listy*, S/102 (2008), pp. 880-881.
- [8] RAHMANI, K. & NATEGH, S. *Mater. Sci. Eng.* Vol. A486 (2008), p. 686.
- [9] STEKOVIC, S. & ERICSSON, T. & JOHANSSON, S. In *Fatigue 2006*. In Control Productions, Monterey, CA, 2006, CD ROM No. FT113.

- [10] JULIŠ, M. & OBRTLÍK, K. & POSPÍŠILOVÁ, S. & PODRÁBSKÝ, T. & POLÁK, J. Effect of Al-Si diffusion coating on the fatigue behavior of cast Inconel 713LC at 800 degC. *Procedia Engineering*, 2 (2010), pp. 1983-1989.
- [11] KRUML, T. & HUTAR, P. & OBRTLÍK, K. & PETRENEC, M. Modelling of damage accumulation under cyclic loading. Study of nucleation and propagation of fatigue cracks. Comparison of physically short cracks against macroscopic cracks under cyclic fatigue. Brno: IPM, 2007.
- [12] SIH, G.C. *Handbook of stress intensity factors*. Institute of Fracture and Solid Mechanics, Lehigh University, Bethlehem 1973.
- [13] SONSINO, C. & M., BRANDT, U. & BERGMANN, J. Fatigue and short crack propagation behaviour of cast nickel base alloys IN 713 C and MAR-M-247 LC at high temperatures. In *Low cycle fatigue and elasto-plastic behaviour of materials - 3*, Elsevier Applied Science, London and New York 1992.
- [14] JACOBSSON, L. & PERSSON, C. & MELIN, S.: *In-situ ESEM study of thermo-mechanical fatigue crack propagation*. Mater. Sci. and Eng. A, 496, (2008) 200-208.
- [15] OBRTLÍK, K. & POLÁK, J. Fatigue growth of surface cracks in the elastic-plastic region. *Fatigue Fract. Eng. Mater. Struct.*, 8 (1985) 23-31.

This research was supported by the Czech Science Foundation (project No. 106/09/P522), by the Ministry of Education, Youth and Sports of the Czech Republic (project Mobility of CZ-SK researchers MEB0810123), by Ministry of Industry and Trade (project No. FR-TII/099), by the Academy of Sciences of the Czech Republic (project No. AV0Z 20410507) and by specific research BUT (project No. FSI-S-10-46).